Eur. J. Biochem. **271**, 4909–4920 (2004) © FEBS 2004 doi:10.1111/j.1432-1033.2004.04460.x

Structure, expression and regulation of the cannabinoid receptor gene (*CB1*) in Huntington's disease transgenic mice

Elizabeth A. McCaw, Haibei Hu, Geraldine T. Gomez, Andrea L. O. Hebb, Melanie E. M. Kelly and Eileen M. Denovan-Wright

Department of Pharmacology, Dalhousie University, Halifax, Nova Scotia, Canada

Loss of cannabinoid receptors (CB1) occurs prior to neurodegeneration in Huntington's disease (HD). The levels and distribution of CB1 RNA were equivalent in 3-week-old mice regardless of genotype demonstrating that the specific factors and appropriate chromatin structure that lead to the transcription of *CB1* were present in the striatum of young R6/2 and R6/1 transgenic HD mice. The expression of the mutant *HD* transgene led progressively to decreased steady-state levels of CB1 mRNA in neurons of the lateral striatum, which was dependent on the size of the CAG repeat and relative expression of the gene encoding mutant huntingtin (*HD*). Although it is known that the coding region of *CB1* is contained within a single exon in mice, rats and humans, the 5′-untranslated region of the mouse gene remained to be defined. CB1 mRNA is encoded by two exons separated by an 18.4-kb intron. Transcription of *CB1* occurred at multiple sites within a GC-rich promoter region upstream of exon 1 encoding the 5′-UTR of CB1. There was no difference in the selection of specific transcription initiation sites associated with higher levels of CB1 expression in the striatum compared to the cortex or between the striata of wild-type and HD transgenic mice. The progressive decline in CB1 mRNA levels in R6 compared to wild-type mice was due to decreased transcription, which is consistent with the hypothesis that mutant huntingtin exerts its effects by altering transcription factor activity. The cell-specific conditions that allow for increased transcription of *CB1* in the lateral striatum compared to other forebrain regions from all transcription start sites were affected by the expression of mutant huntingtin in a time-dependent manner.

Keywords: mutant huntingtin; striatum; transcription initiation sites; quantitative PCR.

Huntington's disease (HD) is a progressive neurodegenerative disorder, characterized by a decline in motor function and cognition, as well as the development of psychiatric symptoms [1]. HD develops when an individual inherits one copy of the *HD* gene with an extended polyglutamine-encoding CAG repeat [2]. The number of CAG repeats is inversely correlated with the age of onset of the disorder [3]. The extended polyglutamine tract in mutant huntingtin confers an abnormal function that ultimately causes neurodegeneration of a subpopulation of cells in the basal ganglia. In addition, a reduction in the level of normal huntingtin may also be detrimental to the survival and function of neurons [4,5].

One of the earliest known changes in human HD patients is the loss of cannabinoid receptors [6]. Immunohistochemistry and radio-ligand binding assays of post-mortem human brains at different ages and stages of HD have demonstrated that CB1 receptors decrease on nerve terminals in the globus pallidus [7] and substantia nigra [6,8] prior to cell loss. Similarly, CB1 mRNA levels decline in the striatum of transgenic HD mice [8,9]. The mechanism by which mutant huntingtin causes changes in CB1 mRNA levels has not yet been determined and it is not known whether the decline in CB1 mRNA levels is caused by decreased transcription, altered mRNA processing or increased mRNA turnover.

There are a number of transgenic mouse models of HD. The R6 transgenic HD mouse models were created by inserting exon 1 of the human *HD* gene, containing an expanded CAG repeat under the control of the human *HD* promoter, into the mouse genome. These transgenic mice do not exhibit neuronal degeneration, but do display a progressive HD phenotype including tremor and abnormal movement characteristic of the symptoms exhibited by human HD patients [10]. R6 mice model early changes in brain function caused by the expression of exon 1 of mutant human huntingtin in animals that have a full complement of mouse huntingtin. Transgenic R6 mouse models differ in the length of the CAG repeat within exon 1 of the human *HD* transgene and site of transgene integration. The R6/1 model has approximately 115 CAG repeats, while the R6/2 model has ≈ 150 repeats. The R6/2 model also has an earlier onset of symptoms and exhibits more severe symptoms than the R6/1 model [10,11]. This observation is consistent with

Correspondence to E. Denovan-Wright, Department of Pharmacology, Sir Charles Tupper Medical Building, 15D Dalhousie University, Halifax, NS, Canada B3H 1X5. Fax: +1 902 494 6294, Tel.: +1 902 494 1363. E-mail: emdenova@dal.ca

Abbreviations: HD, Huntington's disease; CIP, calf intestinal phosphatase; TAP, tobacco acid pyrophosphatase; M-MLV, Moloney murine leukaemia virus; GAPDH, glyceraldehyde-3-phosphate dehydrogenase; qRT, quantitative reverse transcription; HPRT, hypoxanthine ribosyl transferase; RLM, RNA ligase-mediated; EST, expressed sequence tag; RPA, RNase protection assay.

(Received 27 July 2004, revised 4 October 2004, accepted 25 October 2004)

the negative correlation between age of onset and CAG repeat length observed in humans.

Using the R6 transgenic mice as models of early stage HD, we initiated studies aimed at understanding how mutant huntingtin leads to cell-specific dysregulation of the levels of CB1 mRNA. The overall goal of this research was to determine how expression of mutant huntingtin selectively alters the steady-state mRNA levels of specific transcripts such as CB1 in striatal neurons. Since it is known that the length of the CAG repeat affects the onset of HD in humans and in mice, we first confirmed that the rate of decrease in steady-state CB1 mRNA was dependent on the length of the CAG trinucleotide (nt) repeat and relative expression of the *HD* gene. We then determined the structure of the mouse *CB1* gene and determined that transcription of the *CB1* gene was affected in striatal neurons of transgenic HD mice.

Experimental procedures

Animals

Two transgenic HD mice colonies were established and maintained by crossing hemizygous R6/2 or R6/1 males with CBAxC57BL/6 females. Mice were originally purchased from The Jackson Laboratory (Bar Harbor, ME, USA). All mice were genotyped as described previously [12]. Animal care and handling protocols were in accordance with the guidelines detailed by the Canadian Council on Animal Care and were approved by the Carleton Animal Care Committee at Dalhousie University.

In situ hybridization analysis

In situ hybridization was performed on coronal sections (Bregma +1.70 to −0.50 [13]); of 3 to 24-week-old mouse brains using a radiolabeled antisense CB1-specific oligonucleotide probe (MMCB1: 5′-ATGTCTCCTTTGAT ATCTTCGTACTGAATGTCATTTG-3′) as described previously [9]. MMCB1 is complementary to nucleotides 74–110 of the mouse CB1 cDNA (GenBank Accession Number U40709). Nucleotide 1 of this cDNA sequence corresponds to the start of the initiation codon in the CB1 coding sequence shown in Fig. 4. Slides were exposed to Kodak Biomax MR film for 2–4 weeks at room temperature. The CB1 mRNA levels were analysed using KODAK 1D IMAGE ANALYSIS SOFTWARE. The levels of CB1-specific hybridization signal in the lateral striatum were normalized by subtracting the optical density of the CB1-specific hybridization in the medial striatum. The levels of *CB1* mRNA were low in the medial striatum relative to the lateral striatum and were equivalent in all wild-type and HD mice examined. The optical density of the corrected hybridization signal in the lateral striatum was subjected to two-way ANOVA assessing the influence of genotype (WT, R6/1 and R6/2) and age (3–24 weeks) of independent groups of mice ($n = 4$ per specific age and genotype). The overall two-way ANOVA was followed by one-way ANOVAS to assess: (a) the influence of genotype (WT, R6/1, R6/2) on CB1 mRNA levels for each age to determine genotype-specific changes; and (b) the influence of age for each genotype to identify any decreases in CB1 mRNA levels that occurred with increasing age independent of genotype. Tukey's honestly significant multiple comparisons were used to identify alterations in *CB1* gene expression among WT, R6/1 and R6/2 mice at specific ages previously identified by one way ANOVAS as hosting significant genotype- or age-specific differences. A 0.05 level of significance was adopted for all comparisons. The rate of decline in CB1 mRNA levels in R6/2 and R6/1 mice was fit with the equation $y = y° + ae^{-bx}$ using SIGMA PLOT software. The variables which describe the exponential decay in CB1 mRNA levels in R6/2 mice include $y° = 8.72$, $a = 2.8898$ and $b = -0.76$. For R6/1 mice, the variables which describe the exponential decay in CB1 mRNA levels are $y° = 10.39$, $a = 48.87$ and $b = -0.17$. The *P*-value for each coefficient was < 0.01.

5′-RNA ligase-mediated-RACE (5′-RLM-RACE)

To obtain RNA, mice were deeply anaesthetized using sodium pentobarbital (65 $mg \cdot kg^{-1}$ i.p.), decapitated, and cortical and striatal tissue was dissected. The tissue was immersed in liquid nitrogen and stored at −70 °C prior to RNA extraction using Trizol™ (Invitrogen). The First Choice™ RLM-RACE kit (Ambion) was used to prepare a cDNA library. Briefly, total RNA was treated with calf intestinal phosphatase (CIP) to remove the 5′-phosphate from all RNAs that did not have a 7-methylguanosine cap, as well as from any trace genomic DNA. The RNA was then divided into two samples. One aliquot was exposed to tobacco acid pyrophosphatase (+TAP) to remove 7-methylguanosine caps from the 5′-end of the mature mRNAs leaving a free 5′-phosphate. The other aliquot did not receive TAP treatment (–TAP) and served as a control for the effectiveness of the initial CIP treatment. Adapter RNA was ligated to the 5′-phosphate groups on +TAP and control (–TAP) RNA using T4 RNA ligase. Moloney murine leukaemia virus (M-MLV) reverse transcriptase and random decamers were used to synthesize single-stranded cDNA. 5′-RLM-RACE PCR was performed using an outer adapter primer (5′-GCTG ATGGCGATGAATGAACACTG-3′) and MMCB1. An aliquot of the primary PCR reaction was used as the template for a second round of amplification with an inner adapter primer (5′-CGCGGATCCGAACACTGC GTTTGCTGGCTTTGATG-3′) and either MMCB1 or RPAAS (5′-GGTCAGTAAGTCAGTCGGTCTGCG-3′). PCR conditions for both the first and second rounds of amplification using MMCB1 were: 94 °C for 3 min, followed by 35 cycles of 94 °C for 30 s, 60 °C for 30 s, 72 °C for 30 s, followed by a final extension of 72 °C for 10 min. The PCR conditions using RPAAS were identical with the exception that the annealing temperature was increased to 62 °C and the extension time was increased from 30 to 60 s. Aliquots of the secondary PCR reactions were fractionated on a 2% (w/v) agarose gel. The remainder of the PCR-amplified DNA was ligated into TOPO-Blunt™ vector and used to transform TOP10 cells (Invitrogen). The sequence of 20 individual clones was determined by T7 dideoxy sequencing (USB), using [^{33}P]dATP[αP] (3000 $Ci \cdot mmol^{-1}$) and M13 universal forward and reverse primers. The intron and exon sequences of the *CB1* gene were identified by comparing the sequence of the 5′-RLM-RACE cDNA clones to that of

mouse genomic DNA in the database at the Wellcome Trust Sanger Institute. PCR was used to amplify the portion of mouse genomic DNA that was missing in the Sanger database. The CB1 cDNA (AY522554) and genomic DNA (AY522555) sequences were submitted to GenBank.

RNase protection assay

Two probe templates were generated by PCR amplification of mouse genomic DNA containing the putative CB1 transcription start sites that were identified by 5′-RLM-RACE. The downstream probe (RPA-1, Fig. 2B) was created from a sense primer (RPA S: 5′-CGCAGACCG ACTGACTTACTGACC-3′), and an antisense primer (Intron AS: 5′-CCTGGAACACGGAGCAAGAAC-3′) complementary to a sequence within the 5′–end of the intron sequence. The upstream probe (RPA-2, Fig. 2B) was generated from a sense primer (Up2 S: 5′-CCAA TGTCAGGTCAGTTCTTAGGCTCATTAA-3′) complementary to the region upstream of the putative start sites, and an antisense primer (RPAAS) that was complementary to the sense primer of the downstream probe. The PCR cycling parameters were identical to those used for 5′-RLM-RACE with the exception that the annealing temperature was 55 °C and the extension time was 90 s. The 414- and 316-bp PCR products were gel purified using a gel extraction kit (Sigma, Oakville, ON, Canada), cloned in pGEM-T (Promega, Madison, WI, USA) and sequenced. The Lig'nScribe^{TM} kit (Ambion, Austin, TX, USA) was used to generate products that would produce biotinylated CB1-specific antisense RNA after *in vitro* transcription (Maxiscript; Ambion). Two control antisense templates, mouse glyceraldehyde-3-phosphate dehydrogenase (GAPDH) and mouse β-actin (Ambion), were also transcribed *in vitro*. Full-length biotin-labelled ribonucleotide probes were fractionated on a 5% polyacrylamide gel, visualized using UV shadowing, excised from the gel and eluted. The CB1-, GAPDH-, and β-actin-specific probes were stored at −80 °C.

RNase protection assays were performed using the Supersignal RPA III kit (Pierce, Rockford, IL, USA) and striatal and cortical RNA samples from 9-week-old wild-type and R6/2 mice. Each probe (400 pg) was combined with 1, 10 or 25 μg RNA and, following precipitation and resuspension in buffer, allowed to hybridize overnight at 42 °C. Control reactions included 10 pg probe only, and 400 pg probe with excess yeast RNA. After hybridization, all samples, except the sample containing 10 pg CB1 probe only, were subjected to a 30-min RNase digestion using a 1 : 100 dilution of RNase A/T1. Digestion products and a biotinylated RNA ladder (Ambion) were fractionated on a 5% polyacrylamide gel, and transferred to Hybond N+ membrane (Amersham Pharmacia, Piscataway, NJ, USA). Bands were visualized by chemiluminescent detection (Pierce) of the protected probe and RNA ladder.

Quantitative RT-PCR

Quantitative reverse transcription-PCR (qRT-PCR) was used to determine the number of copies of mature and unspliced CB1 transcripts in cDNA samples derived from the striatum of wild-type and HD transgenic mice. Striatal RNA was extracted from 3-, 5-, 6-, and 12 week-old wild-type and R6/1 transgenic HD mice ($n = 6$ per age and genotype). Three gene-specific primers and M-MLV reverse transcriptase (Promega) were used to generate first-strand cDNA using 1 μg total RNA. These primers included Intron AS, MMCB1 and a primer complementary to hypoxanthine ribosyl transferase (HPRT AS: 5′-CACA GGACTAGAACACCTGC-3′). The CB1-specific sense primer used in qRT-PCR reactions corresponded to nucleotides +433 to +454 (RT sense 5′-TCCTTGTAG CAGAGAGCCAGCC-3′) within exon 1 (Fig. 4), which was downstream of the transcription start sites identified by 5′-RLM-RACE within exon 1. This primer was used in conjunction with the coding region-specific antisense primer (MMCB1) to amplify a 253-bp product from cDNA corresponding to mature CB1 transcripts. The RT sense primer was also used with the Intron AS primer to amplify a 192-bp product from unspliced CB1 primary transcript. *HPRT* was amplified using HPRT AS and HPRT S (5′-GCTGGTGAAAAGGACCTCT-3′) primers. Standards, containing 10^6 to 10^1 copies of PCR products derived from mature and primary CB1 mRNA and HPRT mRNA were prepared. qRT-PCR was performed following the manufacturer's instructions for LightCycler DNA FastStart SYBRGreen 1 [14] using 5 mM $MgCl_2$ for amplification of *HPRT*, 4 mM $MgCl_2$ for amplification of mature CB1 cDNA, and 2 mM $MgCl_2$ for amplification of primary CB1 cDNA. Quantitative PCR was performed simultaneously on individual cDNA samples and known amounts of each standard using each set of primers. HPRT cycling conditions were 10 min at 95 °C, 45 cycles of denaturation (95 °C for 15 s), annealing (63 °C for 5 s), and extension (72 °C for 10 s). Fluorescence was quantified at the end of each cycle. Annealing temperature was reduced to 60 °C to amplify primary and mature CB1 cDNA. As negative controls, the reverse transcriptase enzyme was omitted from cDNA synthesis reactions for each sample and –RT controls were subjected to qRT-PCR. No products were observed in –RT reactions using primers for HPRT and mature CB1 mRNA. Small amounts of product were observed in some, but not all, reactions containing CB1 primary transcript-specific primers, which corresponded to trace genomic DNA. The amount of product in the –RT reactions was subtracted from the amount of product in each +RT reaction and the amount of primary and mature CB1 transcript was normalized by dividing by the amount of HPRT in each sample.

Results

CB1 mRNA levels decline at different rates in two strains of transgenic HD mice

In situ hybridization was performed on coronal brain sections of wild-type, R6/1 and R6/2 mice, ranging in age from 3 to 24 weeks (Fig. 1). The highest levels of CB1-specific hybridization were observed in the lateral striatum of wild-type mice and 3-week-old R6/1 and R6/2 transgenic HD mice (Fig. 1A). The CB1-specific hybridization signal was decreased in the lateral striatum of older transgenic HD mice. There was no statistically significant change in CB1

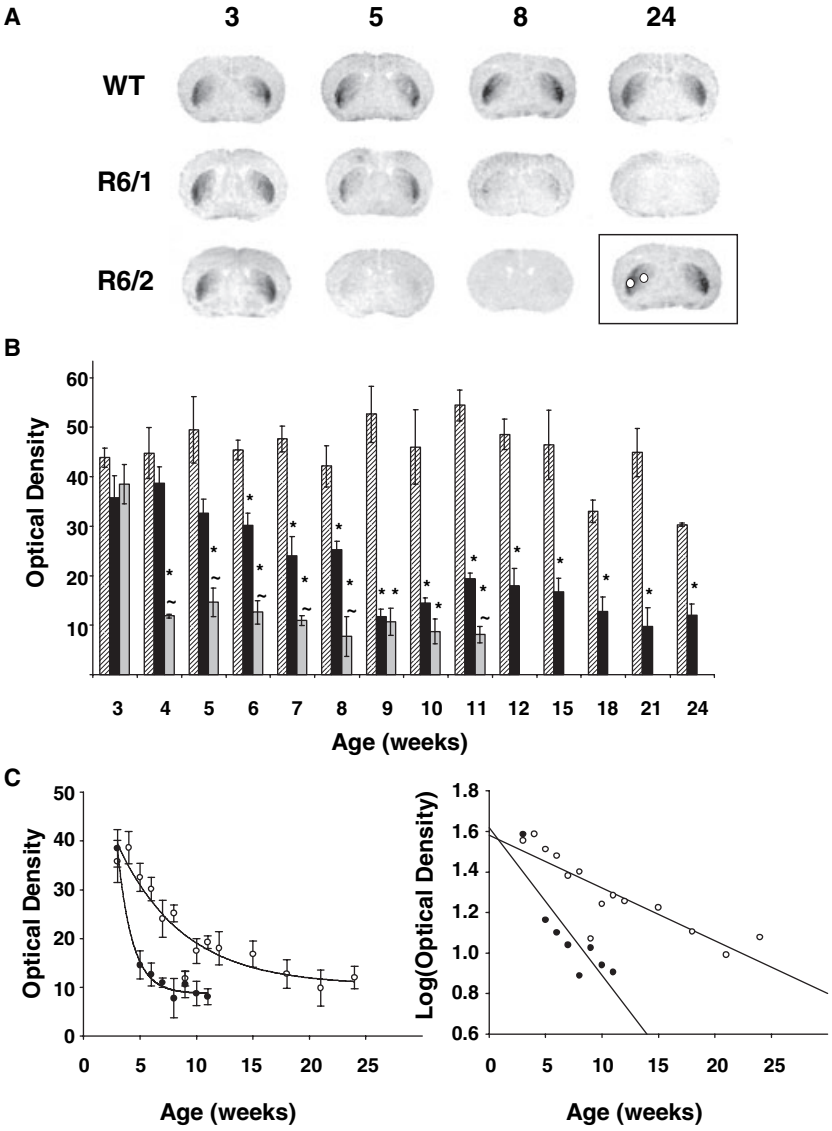

Fig. 1. The progressive decrease in the steady-state CB1 mRNA levels in the lateral striatum of HD mice is dependent on genotype. (A) Representative mouse brain sections subjected to *in situ* hybridization to detect CB1 mRNA using the MMCB1 probe. The most intense hybridization signal is seen in the lateral striatum of the brains, which remained constant in the wild-type (WT) mice and decreases over time in the R6/1 and R6/2 mouse brains. The age in weeks of each mouse is indicated above each column showing a representative coronal brain section (Bregma $\approx$ 0.80) for each genotype at selected ages. The white circles on the inset (boxed) section derived from an 8-week-old wild-type mouse in A represent the regions of each brain that were subjected to densitometric analysis of the CB1-specific hybridization signal. (B) Histogram showing the average optical density ($\pm$ SE of the mean) of the hybridization signal in the lateral striatum for four individual wild-type (striped bars), R6/1 (black bars), and R6/2 (grey stippled bars) mice of each age indicated on the *x*-axis. *Statistical significant difference from WT mice; ~statistical significant difference from R6/1 mice at the identical age. (C) SIGMA PLOT was used to fit the best curve that describes the rate of change in CB1 mRNA levels in the lateral striatum of R6/1 (open circles) and R6/2 (solid circles) mice. The optical density values of the levels of CB1 mRNA in the lateral striatum fit a logarithmic decay curve for both the R6/1 and R6/2 strains of HD mice with a coefficient of determination (R^2) value of 0.99 and 0.88 for R6/2 and R6/1 mice, respectively.

mRNA levels in the medial striatum of any of the wild-type and HD mice examined. The optical density of the hybridization signal in the lateral striatum, corrected by subtracting the signal in the medial striatum, of four mice per age and genotype were averaged (Fig. 1B), subjected to two-way ANOVA and *post hoc* tests. There was no significant change in the steady-state levels of CB1 mRNA in the lateral striatum of wild-type mice from 3 to 24 weeks of age. CB1 mRNA levels in the lateral striatum of R6/2 HD mice decreased from wild-type levels at 3 weeks of age to a minimum level of $\approx$ 30% of that observed in wild-type mice by 4 weeks of age ($P < 0.05$) and remained constant at all other time points examined. The minimum level of CB1-specific *in situ* hybridization signal observed in older R6 mice corresponds to CB1 mRNA levels that do not continue to decline to less than $\approx$ 30% of the levels observed in wild-type mice because minimum levels of CB1 mRNA are detected by Northern blot analysis of RNA samples derived from the cortex of wild-type and the cortex and striatum of R6/2 HD mice [9]. CB1 mRNA levels in the lateral striatum began to decrease at 5 weeks in R6/1 mice, reached a minimum level by 9 weeks ($P < 0.05$) and remained relatively constant over the next 15 weeks. There was no statistically significant difference in the amount of CB1 mRNA detected in the oldest R6/2 (11 weeks) and R6/1 mice (24 weeks). The age-dependent decrease in the average steady-state levels of CB1 mRNA in the lateral striatum of the two transgenic HD mouse strains fit simple exponential decay curves (Fig. 1C). This data indicated that the rate of change in the levels of CB1 mRNA in the lateral striatum was dependent on age and genotype.

Previously, we determined that CB1 mRNA is highly expressed in isolated neurons in the cortex and hippocampus of wild-type mice [9]. Most cells of the cortex express CB1 at levels that are similar to that observed in the medial striatum. The levels of CB1 mRNA in the medial striatum and majority of cortical neurons remained constant in wild-type and R6/1 and R6/2 transgenic HD mice. Isolated neurons that had high levels of CB1 mRNA expression were visible in the cortices of all wild-type mice, all 3 to 15-week-

old R6/1 and all 3 to 7-week-old R6/2 mice examined (data not shown). In contrast, we did not observe isolated cortical neurons with high levels of CB1 expression in any 18 to 24-week-old R6/1 or 9 to 12-week-old R6/2 mice. We did observe labelling of isolated cortical neurons with increased CB1 mRNA levels in all 8-week-old R6/2 mice examined although the number of these neurons appeared to be reduced in 8-week-old R6/2 compared to 3 to 7-week-old R6/2 and wild-type mice. The random distribution and paucity of these neurons, however, precluded an accurate quantitative comparison of the number of neurons in the cortex among mice of different ages and genotypes.

The *in situ* hybridization analyses demonstrated that CB1 mRNA levels in the lateral striatum and isolated cortical neurons, but not in the medial striatum or the majority of cells in the cortex, declined at different rates in two strains of transgenic HD mice. In addition, expression of CB1 in the lateral striatum was affected prior to the time that expression of CB1 in isolated cortical neurons was affected in both strains of R6 transgenic HD mice. It appeared that the amino terminus of mutant huntingtin containing an expanded polyglutamine tract caused the steady-state CB1 mRNA levels in the lateral striatum to decrease between 3 and 4 weeks and 5 and 9 weeks in R6/2 and R6/1 mice, respectively, and that mRNA levels in the lateral striatum reached a new constant level that was similar to that observed in the medial striatum and cortex. These data suggested that either the rate of CB1 transcription or the relative stability of CB1 mRNA was affected in a manner that was dependent on the length of the CAG repeat and relative expression of the human *HD* transgene in the two strains of mice and that mutant huntingtin differentially affected CB1 mRNA levels in specific types of neurons.

Mus musculus CB1 gene structure

The coding region of *CB1* is contained within a single exon in mice, rats and humans [15–17]. However, the 5′-untranslated region of the mouse gene remained to be defined. As a first step in defining the *CB1* promoter, we determined the sequence and structure of the 5′-end of cDNAs corresponding to full-length mature CB1 mRNA and deduced the structure of the *CB1* gene by comparing the cDNA sequences to the genomic DNA sequences available in the mouse genome sequence database at the Sanger Wellcome Trust Institute. 5′-RLM–RACE was performed to identify the 5′-end of 7-methylguanosine-capped CB1 mRNAs expressed in the striatum of wild-type mice. PCR amplification was performed using a CB1-specific primer complementary to a sequence within the coding region of CB1 (MMCB1). The PCR products were between 50 and 400 bp in length. Abundant products greater than 200 bp were not visible in the –TAP control sample (Fig. 2A). The PCR products from the +TAP reactions were cloned and the cloned inserts ranged in size from 100 to 450 bp. The sequence of several clones for each insert size was determined and the sequences were aligned with mouse genomic DNA (Wellcome Trust Sanger Institute database). In each clone, the cDNA sequence was colinear with the genomic sequence from 62 bp upstream from the CB1 translation start site until the 3′-end of MMCB1. The remainder of the sequence of each clone corresponded to the 5′-untranslated region of CB1 mRNA, which was colinear with mouse genomic sequence 18.4 kb upstream of the coding region of the *CB1* gene. Because the genomic sequence of this region was incomplete in the Sanger database, we used PCR to amplify the ambiguous region and compared genomic and cDNA CB1 sequences. The 5′-UTR of the mouse *CB1* gene contained an 18 406 bp intron with conserved intron splice site sequences (Fig. 2B). Because the PCR reactions may have preferentially amplified small products, a second gene-specific primer (RPAAS) was used in 5′-RLM-RACE reactions (Fig. 2A) to determine if any CB1 transcripts had 5′-ends upstream of those determined using the primer complementary to the coding region of CB1. One product of $\approx$250 bp was cloned and sequenced. In total, seven different sized 5′-RLM-RACE clones with unique 5′-ends were identified, which corresponded to seven putative transcription initiation sites within the *CB1* gene upstream of the intron in the 5′-UTR. It is unlikely that premature termination of the reverse transcriptase reaction could generate the 5′-end of these cDNAs as the adapter sequence was present in each cloned insert and the adapter RNA was added before the reverse transcriptase reaction. Several expressed sequence tags (EST) and cDNA CB1 clones have been listed in GenBank that contain sequence on both sides of the CB1 intron. Each of these ESTs have a unique 5′-end compared to those determined by 5′-RLM-RACE (Fig. 2B). We have designated the +1 position of exon 1 as the 5′ most transcription start site identified using 5′-RLM-RACE. Other CB1 cDNA sequences in GenBank (U40709, BE650953, U17985) have 5′-ends that are 3′- to the CB1 intron. Unlike the 5′-RLM-RACE cDNA clones, these EST clones may have resulted from premature termination of reverse transcriptase reactions or they may represent additional CB1 transcription start sites. The putative transcription initiation sites of the mouse *CB1* gene are shown in Fig. 2B and Fig. 4.

The human *CB1* gene described in the Sanger database has two exons separated by an intron. The relative position of the introns in the mouse and human genes are identical and the sequences at the 5′- and 3′-splice site junctions are conserved and correspond to splice junction consensus sequences (Fig. 2B). There are two human CB1 cDNA clones reported in GenBank (X54937 and NM_001840) that have the same 5′-end. The position of the transcription start site for human CB1 does not correspond to any of the start sites identified in the mouse *CB1* gene (Fig. 4). In both mouse and human, the upstream region of *CB1* is GC rich as would be predicted for a promoter region. There is a putative TATA box (CATAAAT) 25 bp upstream of the +1 transcription start site in the mouse *CB1* gene. Conserved TATA boxes are not found within 25 bp of the human or other mouse transcription start sites.

Decreased transcription of *CB1* in HD mice

Because of the apparent complexity in the number of transcription initiation sites in the mouse *CB1* gene and because 5′-RLM-RACE may have led to the identification of rare copies of mRNA, we decided to determine whether the 5′-transcription initiation sites could be observed without using a PCR-based detection method. RNase

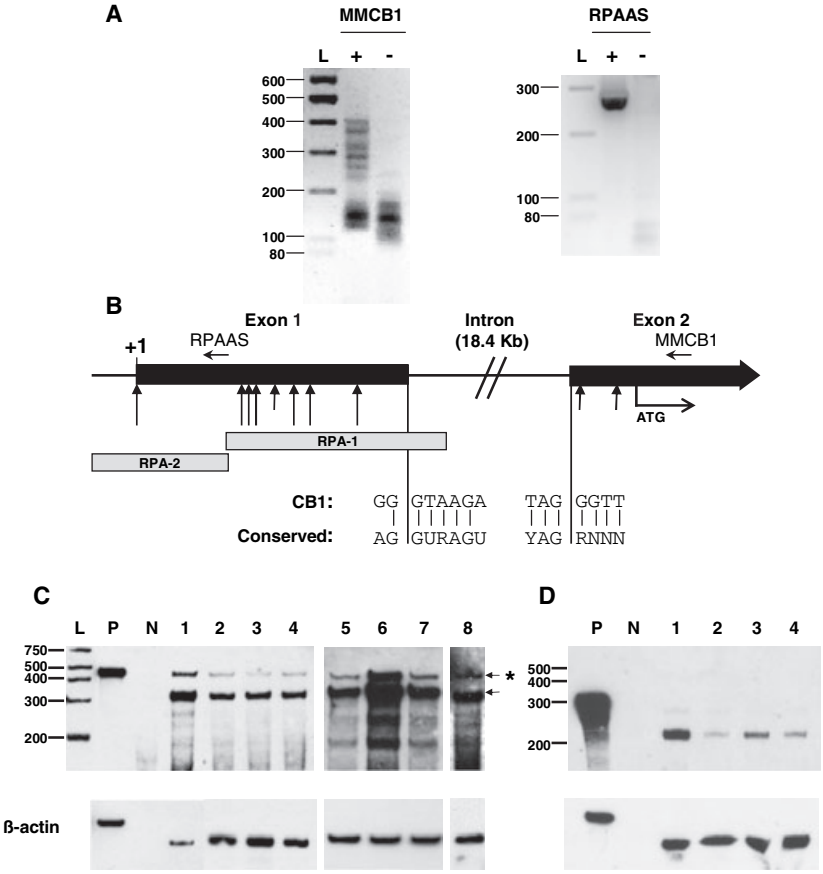

Fig. 2. Transcription initiates at multiple sites upstream of the intron within the 5′-untranslated region of the *CB1* gene. (A) 5′-RLM-RACE was performed using *CB1* gene-specific primers 1 and 2 (MMCB1 and RPAAS). Products were fractionated on 2% agarose gels. The size of molecular mass markers (100 bp ladder, L) is indicated on the left of each gel. The control reaction (–TAP) is indicated by -, and the experimental products (+TAP) are indicated by +. The +TAP-specific PCR products were cloned and sequenced. (B) The large upward pointing arrows indicate the relative positions of the 5′-ends of the cDNA clones identified by 5′-RLM-RACE compared to the exon/intron organization of the *CB1* gene. The major transcription initiation site is indicated by +1 (Fig. 4). The small upward pointing arrows indicate the 5′-end of mouse CB1 EST and cDNA clones found in GenBank. The relative position of MMCB1 and RPAAS used for 5′-RLM-RACE are indicated. The sequence corresponding to conserved splice sites [35] is aligned below the corresponding sequence of the mouse *CB1* gene at the intron–exon junctions and the approximate size of the intron separating the two *CB1* exons is 18.4 kb. The relative positions of RPA-1 and RPA-2 probes used for RPA analysis (C and D) are shown. For each series of protection reactions, 10 pg of undigested probe control (P) and a no target control that consists of 400 pg of probe combined with excess yeast RNA and digested with RNase (N) are shown. In C, 10 μg wild-type striatal RNA (lane 1), 25 μg R6/2 striatal RNA (lane 2), 25 μg wild-type cortical RNA (lane 3) and 25 μg R6/2 cortical RNA (lane 4) were subjected to RPA using the RPA-1 probe. The RNA samples were all derived from 9-week-old mice. Each of the RPA-1-specific products were detected in an over-exposure of an RPA analysis of 25 μg wild-type cortical (lane 5), wild-type striatal (lane 6), R6/2 striatal (lane 7) and R6/2 cortical (lane 8) RNA. The arrow to the right of lane 8 indicates the most abundant protected product observed in all samples. The RPA product corresponding to unspliced primary transcript is indicated by an arrow and asterix. The relative mobility of biotin-labelled RNA ladder (L) is indicated to the left of each blot. A 1 μg aliquot of each RNA sample shown in (C) and (D) was subjected to RPA using the β-actin-specific RPA probe and are shown beneath each blot. In (D) the RPA-2-specific product was detected in 10 μg of 18-week-old wild-type striatal RNA (lane 1), R6/1 striatal RNA (lane 2), wild-type cortical RNA (lane 3) and R6/1 cortical RNA (lane 4).

Protection Assays (RPA) were conducted to confirm the position of the transcription start sites identified by 5′-RLM-RACE reactions and to determine the relative abundance of mRNAs with specific 5′-ends. Mouse β-actin- and GAPDH-specific probes were prepared and used as controls in the RPA assays. β-actin levels are not affected by the expression of exon 1 of mutant *HD* [18] and the amount of protected β-actin-specific probe was used to normalize the amount of input RNA in all other experiments (Fig. 2C). GAPDH mRNA decreases in the striata of symptomatic transgenic R6/2 HD compared to wild-type mice [19]. GAPDH was used as a positive control to demonstrate that RPA could detect differences between the amount of mRNA in wild-type and transgenic HD RNA samples. Levels of GAPDH mRNA, normalized to β-actin mRNA, were ≈ 50% lower in 9-week-old R6/2 compared to wild-type mice (data not shown). Two controls were included in each RPA experiment. The first control included probe that was not hybridized with target RNA or treated with RNase. The second control included RNase-treated

probe in the presence of excess yeast RNA. The former control demonstrated that the probe was full-length and the latter control demonstrated that the probe was only protected if it annealed with complementary mRNA and was protected from RNase digestion.

We hypothesized that the differences in steady-state CB1 mRNA levels between the lateral striatum and cortex and between the lateral striata of control and R6 HD mice may have been due to differences in transcription start site usage. To determine whether the decline in CB1 mRNA levels in transgenic HD mice was related to differences in transcription initiation start site selection, RPA was conducted using RNA isolated from the striatum and cortex of wild-type and R6/2 animals. A 425-bp probe (RPA-1) was synthesized that spanned the mouse genomic DNA sequence containing the majority of the putative transcription initiation sites upstream of the *CB1* intron. This probe was created from a 414-bp PCR product corresponding to a region of genomic DNA extending from between the first and second putative transcription initiation sites within exon 1, to 110 bp into the 5′-end of the intron (Fig. 2B). In the 9 week-old wild-type and R6/2 transgenic mouse striatal RNA samples, the most abundant RPA product was 320 nts in length, which corresponded to the length of the probe that was protected by the exon 1-specific portion of the CB1 mRNA (Fig. 2C). This indicated that the most abundant CB1 mRNAs were produced from a transcription start site or sites that existed at a location upstream of the sequence included in the RPA-1 probe. In addition to the 320-nt protected probe, other less abundant protected fragments were visible. The 150–280 nt fragments corresponded in size to probes that annealed with mRNA that initiated at transcription start sites identified by 5′-RLM-RACE. All of the protected products observed in the wild-type sample were present in both the R6/2 striatal RNA, and the wild-type and R6/2 cortical RNA (Fig. 2C). There was less of each protected product in the R6/2 striatal and cortical RNA samples and in wild-type cortical RNA samples compared to wild-type striatal RNA samples, although it appeared that the relative proportion of each band in any sample remained constant in independent experiments using different amounts of input RNA. There was less of the most abundant 320-nt CB1 mRNA protected product in R6/2 compared to wild-type striatal RNA. The amount of the protected product in the R6/2 striatal sample was equivalent to the amount of the protected product in both the wild-type and R6/2 cortical RNA samples. This analysis demonstrated that there was no striatum-specific use of particular CB1 transcription initiation sites or change in transcription initiation site usage due to the expression of mutant huntingtin.

We also detected a RPA product that was protected after annealing with unspliced primary CB1 transcript. The size of this protected product (414 nts) was slightly less than the full-length CB1 probe (425 nts) although this difference was not apparent on the 5% denaturing acrylamide gels presented in Fig. 2. The 11 nt difference in size between the undigested full-length RPA probe and the CB1 primary transcript-protected product corresponds to adapter sequence added to the CB1 probe during synthesis. No protected products were observed after RNase treatment in reactions containing RPA probe and 1–10 μg genomic DNA (data not shown) demonstrating that the 414-nt protected probe had annealed to primary CB1 mRNA and not contaminating DNA. There was less primary transcript-protected product when 25 μg of R6/2 striatal RNA was used in the hybridization reaction compared to 10 μg of wild-type striatal RNA, suggesting that the levels of unspliced primary CB1 transcript in each sample were proportional to the levels of mature CB1 transcript (Fig. 2C). The amount of primary transcript was lower in R6/2 compared to wild-type striatal RNA and the ratio of the optical density of the primary to mature transcript was ≈ 0.1 in all cortical and striatal RNA samples suggesting that there was decreased transcription of the *CB1* gene in HD mouse brain. This supports the hypothesis that the rate of transcription of CB1 in the striatum of symptomatic R6/2 mice is similar to the rate of transcription in regions of the brain where CB1 is expressed at a low basal level, and that the cell-specific conditions that allow for increased transcription of the *CB1* gene in the lateral striatum compared to other forebrain regions, are time-dependently affected by the expression of mutant huntingtin.

Because it appeared that the majority of transcripts were derived from a start site that was upstream of the 5′-end of the sequence included in RPA-1, we synthesized a second probe (RPA-2) and repeated the RPA analysis of striatal and cortical RNA isolated from wild-type and symptomatic R6 mice. RPA-2 spanned a 314-bp sequence containing the first putative transcription start site (Fig. 2B). These analyses demonstrated that the majority of CB1 transcripts were synthesized from transcription start site 1, which is located 266 bp upstream of the 3′-end of RPA-2. The levels of CB1 mRNA derived from the +1 position (Fig. 4) were lower in all cortical RNA samples and striatal RNA isolated from R6 mice compared to the levels observed in wild-type striatal RNA (Fig. 2D). Therefore, there was one predominant transcription start site and several other transcription start sites in the mouse *CB1* gene that were used to express the *CB1* gene in striatal and cortical neurons. We consistently saw the same pattern of RPA-protected products in wild-type and the two R6 strains of different ages (data not shown). The levels of CB1 mRNA produced from each transcription start site in the striatum of R6 compared to wild-type mice declined proportionately demonstrating that there is no transcription initiation site selection associated with either the expression of CB1 in the striatum vs. the cortex or expression of CB1 in transgenic HD mice.

To test the hypothesis that expression of mutant huntingtin decreased CB1 transcription, we measured the amount of primary and mature CB1 transcript in striatal RNA of wild-type and R6/1 mice by qRT–PCR. R6/1, and not R6/2, mice were used in this study because the rate of CB1 mRNA decline was slower in R6/1 compared to R6/2 mice (Fig. 1B,C) and we hypothesized that it may have been possible to determine whether primary transcript levels changed prior to the time that the decrease in mature CB1 transcript levels were apparent in R6/1 mice. Because intron splicing occurs cotranscriptionally [20], the amount of primary transcript present at a given time point reflects the amount of newly synthesized primary transcript. Relative rates of transcription can therefore be inferred from quantification of primary transcript levels. We isolated

RNA from striata of 3-, 5-, 6- and 12-week-old wild-type and R6/1 mice and prepared cDNA using gene-specific primers complementary to exon 2 and intron 1 of the mouse *CB1* gene. A primer complementary to the mouse HPRT mRNA was also included in the reverse-transcriptase reactions. HPRT is constitutively expressed in wild-type and R6 transgenic mice and the levels of HPRT were used to normalize CB1 levels among samples. Consistent with *in situ* hybridization results, qRT-PCR demonstrated that there was no difference in the amount of mature CB1 transcript in the striatum of 3- and 5-week-old wild-type and R6/1 mice (Fig. 3). While less mature CB1 transcripts were detected in the brains of 6-week and 12-week R6/1 transgenic mice compared to age-matched wild-type mice, this difference was only statistically significant at 12 weeks ($P < 0.05$) (Fig. 3A). The qRT-PCR analysis of mature CB1 mRNA levels differed from our previous *in situ* hybridization results where there was a statistically significant difference in the levels of CB1 mRNA between 6-week-old wild-type and R6/1 mice. However, the *in situ* hybridization results were based on the levels of CB1 mRNA in the lateral striatum where the highest levels of expression of CB1 are found and the mutant huntingtin-induced decline in CB1 occurs. In contrast, the cDNA for qRT-PCR was derived from the entire dissected striatum and, as such, the observed decrease in the CB1 mRNA levels in the striatum of R6 mice was diluted by the amount of message contributed by other striatal neurons where CB1 mRNA levels remained constant.

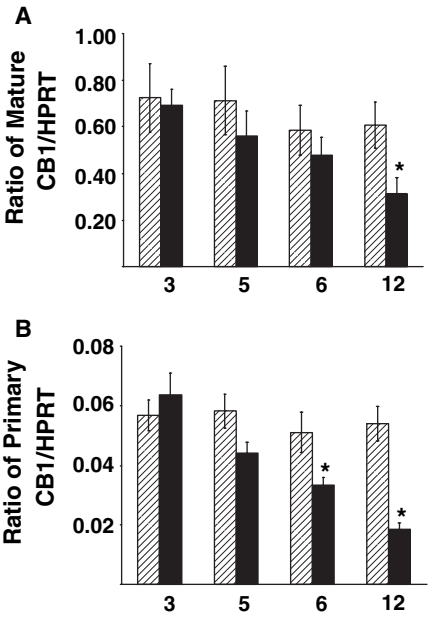

Fig. 3. Primary CB1 transcripts decrease in R6/1 HD mice prior to the loss of mature *CB1* mRNA. Using qRT-PCR, we quantified mature *CB1* mRNA (A) and primary CB1 transcripts (B) from wild-type and R6/1 HD mice striatal RNA. One microgram of total striatal RNA from each sample was used for cDNA synthesis. The levels of CB1 primary and mature transcripts were normalized to the concentration of HPRT in each sample. The ratio of mature (A) or primary (B) CB1 to HPRT is represented on the *y*-axis. The age of the mice in weeks from which the RNA was extracted is indicated on the *x*-axis. The striped and solid bars represent the mean values for wild-type ($n = 6$) and R6/1 ($n = 6$) mice, respectively. Each experiment was performed simultaneously on three samples per transcript, age and genotype and the data were pooled ($n = 6$). The error bars represent SE of the mean. Normalized cDNA levels were subjected to one-way analysis of variance (ANOVA). *Significant difference ($P < 0.05$) from wild-type.

No statistically significant difference was detected in the amount of primary CB1 transcript among wild-type and R6/1 mice at 3 or 5 weeks of age. However, the average primary transcript level was lower in 5-week-old R6/1 compared to wild-type mice. The levels of primary CB1 transcript detected were significantly decreased in the striatum of 6- ($P < 0.05$) and 12-week-old ($P < 0.05$) R6/1 mice compared to age-matched wild-type mice (Fig. 3B). Based on these observations and RPA analysis of primary transcript levels, it appeared that the rate of transcription of the CB1 gene was decreased in the striata of R6 mice and that this decrease led to the observed decrease in steady-state levels of mature CB1 mRNA.

Comparison of human and mouse CB1 promoters

Using MATINSPECTOR (http://www.genomatix.de), several transcription factor-binding sites were detected upstream of the major transcription start site and within the 5′-UTR of the mouse *CB1* gene. Transcription factor binding sites with 100% core sequence similarity and ≥95% matrix similarity are listed in Table 1. We analysd the genomic DNA sequences of the human and mouse *CB1* genes in the region including and upstream of the transcription initiation sites to locate conserved regulatory sequences. The promoter sequences were readily aligned but did contain insertion/deletion differences (Fig. 4). Several transcription factor-binding sites were conserved in the *CB1* promoters of both species (Fig. 4). A number of transcription factors have been shown to physically interact with mutant huntingtin including SP1, NcoR, CREB and NRSF [5,21–24]. Conserved SP1, but not NCoR, CREB and NRSF, binding sites were located in the mouse and human CB1 promoters. No NCoR, CREB or NRSF binding sites with 100% core similarity were observed in the mouse *CB1* region within 500 bp upstream or downstream of the major transcription start site. The identification of the transcription factors that control *CB1* gene expression and which, if any, of these transcription factors interact with mutant huntingtin remains to be determined.

Discussion

The endogenous ligands of CB1, arachidonylethanolamide (anandamide) [25] and 2-arachidonyl glycerol [26], act as modulators of dopamine neurotransmission, and abnormalities in cannabinoid signalling or modulation of dopamine signalling or both have been implicated in a number of neurodegenerative diseases including HD and Parkinson disease, and in other neuropsychiatric disorders such as schizophrenia [27]. Cannabinoid receptors therefore are important modulators of brain function and loss of these receptors would likely negatively impact brain function in HD patients [6]. Our goal, however, was to complete a description of the mouse *CB1* gene and to determine how CB1 mRNA levels are affected in HD transgenic mice as a

Table 1. Transcription factor binding sites in the mouse *CB1* promoter. AREB6, Atp1a1 regulatory element binding factor 6; MZF1, myeloid zinc finger protein; RAR, retinoic acid nuclear receptor; WHN, winged helix protein; BKLF, basic krueppel-like factor; ZF5, zinc finger domain; MYT1, zinc finger TF involved in primary neurogenesis; E2A proteins, and GATA-1, half-site 1; ARNT, AhR nuclear translocator homodimers; CLOCK BMAL, binding site of Clock/BMAL heterodimer; AP1, Activator protein 1; SP1, stimulating protein 1; HMGIY, high-mobility group protein 1; MYOD, Myoblast determining factor; LMO2COM, complex of Lmo2 bound to Tal1, E2A proteins, and GATA-1, half-site 1.

Transcription factor	Core consensus	Number of sites	Positions relative to +1[a]
Sequence			
AREB/AREB6	GGTG	2	−471, +467
ETSF/ELK1	TTCC	1	−471
MZF1/MZF1	CCCC	2	−471, −116
RARF/RAR	GACC	1	−396
CMYB/CMYB	TAAC	1	−348
VMYB/VMYB	AACG	1	−348
WHZF/WHN	ACGC	3	−318, +109, +201
ELKF/BKLF	GGGT	1	−267
ZF5F/ZF5	GCGC	3	−219, −138, +206
MYT1/MYT1	AAGT	1	−153
HIFF/ARNT	CGTG	1	−53
EBOX/MAX	CACG	1	−52
HIFF/CLOCK BMAL1	CGTG	1	−52
AP1F/AP1	TGAC	1	+222
SP1F/SP1	CGCC	1	+260
SORY/HMGIY	TTAA	1	+423
MYOD/MYOD	GGTC	1	+465
MYOD/LMO2COM	CAGG	1	+466

[a] Numbers refer to the position of the 5′-end of the conserved matrix of each response element in relation to the +1 major transcription initiation site in the mouse *CB1* promoter presented in Fig. 4.

first step in defining one of the toxic functions of mutant huntingtin.

The length of the trinucleotide CAG repeat within the *HD* gene is correlated with the time of symptom onset, rate of disease progression and severity of symptoms in HD patients and HD transgenic mice [3,10]. The R6/1 mice have a later age of motor symptom onset and cognitive decline and slower disease progression than the R6/2 mice [10,28]. Previous work demonstrated that levels of mutant huntingtin protein are lower in the R6/1 mice compared to R6/2 [10] and that neuronal intranuclear inclusions (NIIs) containing the human transgene-encoded amino terminus of human huntingtin form more slowly throughout the brain tissue in R6/1 compared to R6/2 mice [29,30]. The differences between the two transgenic lines of HD mice include the length of the CAG repeat within the *HD* transgene and the site of integration of the transgene [10], which appears to lead to differences in the amount of protein produced from the transgene. Therefore, the length of the polyglutamine tract encoded by the human *HD* transgene or relative expression of the transgene affects the rate of HD progression in these mice. To determine whether the rate of decline in steady-state CB1 mRNA levels was dependent on genotype, *in situ* hybridization was used to detect CB1 mRNA in the brains of wild-type and the R6/1 and R6/2 transgenic HD mice. *In situ* hybridization and densitometric analysis demonstrated that the steady-state levels of CB1 mRNA in the lateral striatum of wild-type mice remained constant in 3 to 24-week-old mice but that there was a significant decline in CB1 mRNA in both R6/1 and R6/2 mice. Loss of CB1 mRNA levels in the lateral striatum of R6/2 HD mice occurred at a faster rate, and at an earlier age compared to the R6/1 mice. The final steady-state levels of CB1 mRNA were the same in both strains of R6 transgenic HD mice. Therefore, the relative expression level of mutant huntingtin or length of the CAG repeat or both affected the onset and rate of decline of CB1 mRNA levels. Moreover, because the final steady-state level of CB1 mRNA was the same in both models of transgenic HD mice and the rate of decline of the CB1 mRNA was described by simple exponential decay curves in both species, it appears that the length of the CAG repeat and relative expression of the transgene affected the rate of mRNA message loss but not the final steady-state levels of CB1 mRNA.

We also wished to define the structure of the mouse *CB1* gene and quantify the levels of mRNA that corresponded to each transcription start site in striatal RNA to determine whether there was differential transcription start site usage among tissues or between wild-type and R6 transgenic HD mice. Multiple CB1 transcription start sites were identified upstream of an 18.4-kb intron by 5′-RLM-RACE and confirmed by RNase protection assays. cDNA and EST clones with 5′-ends corresponding to sequences located downstream of the mouse *CB1* intron are present in GenBank. It is possible therefore that transcription may occur downstream of the mouse *CB1* intron although we did not detect any 5′-RLM-RACE clones that corresponded to capped mRNAs that initiated in exon 2. To date, only a single human CB1 transcription start site has been described, which is upstream of the intron in the human *CB1* gene. The single transcription initiation site for human *CB1* does not correspond to any transcription initiation sites identified in the mouse *CB1* gene. The exon/intron organization and primary sequence of the coding and regulatory sequences are conserved between the mouse and human *CB1* genes.

RPA analysis demonstrated that there is a proportional loss of the CB1 transcripts from each of the transcription start sites of the *CB1* gene in R6 transgenic HD compared to wild-type mice. This indicated that specific mRNAs derived from particular start sites were not preferentially lost in the striatum of HD mice. Further, the final equilibrium levels of each CB1 transcript in the striatum of HD mice was the same as the basal levels of CB1 mRNA found in the cortex in both wild-type and HD mice. This conclusion is supported by earlier Northern blot analysis of the levels of CB1 mRNA in the striatum and cortex of wild-type and R6/2 mice [9]. This indicated that the difference between neurons in the medial striatum and cortex that express basal levels of CB1 and neurons in the lateral striatum that have higher steady-state levels of CB1 mRNA, was not due to different start site selection within the *CB1* promoter. It appears that the factors or conditions that control the higher steady-state levels of CB1 mRNA in the lateral striatum compared to the medial striatum and cortex

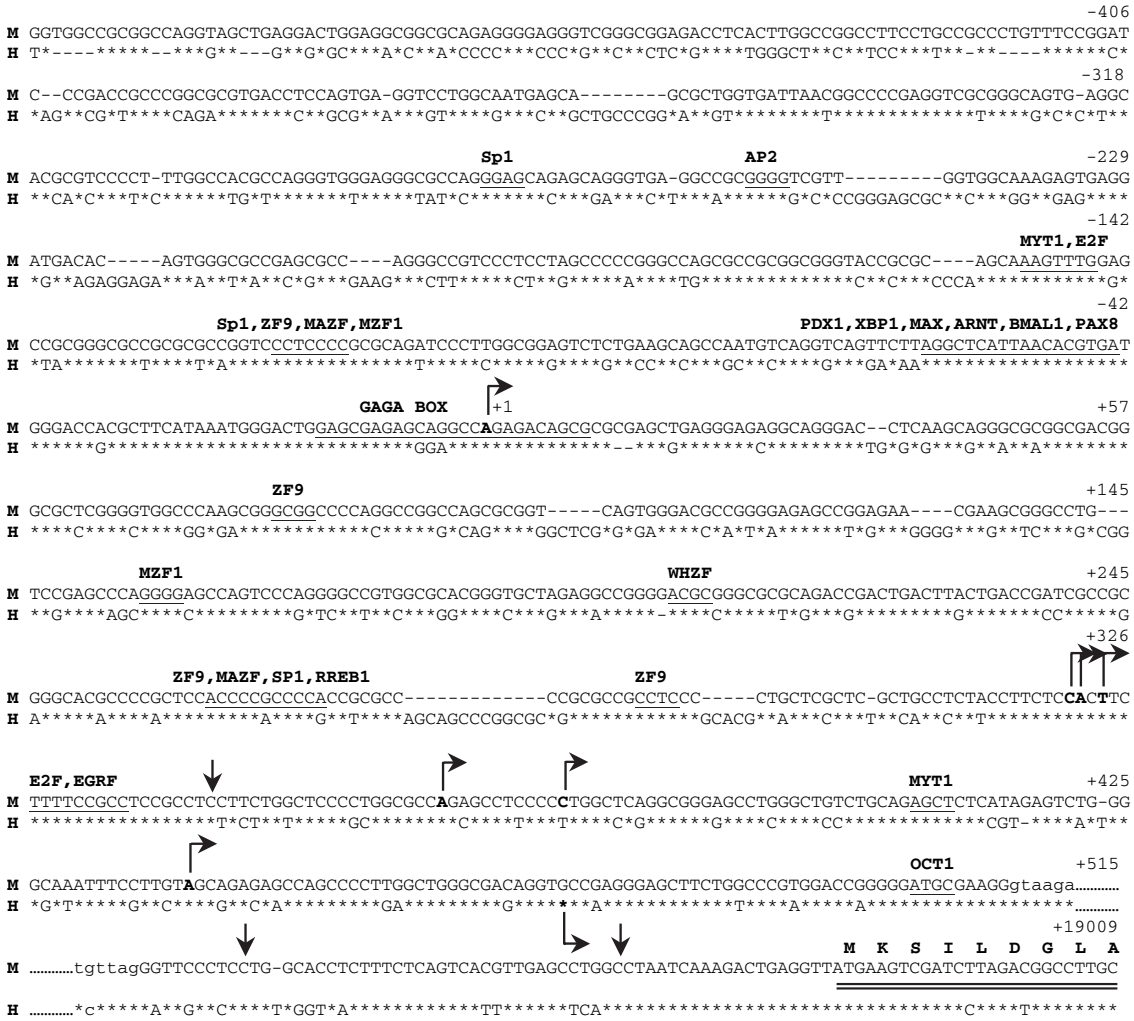

Fig. 4. CLUSTAL alignment of the mouse (M) and human (H) *CB1* promoter regions. Stars represent nucleotides found in the human CB1 genomic DNA that match the mouse DNA sequence. Dashes indicate insertion/deletions. The position indicated by +1 is the major CB1 transcription initiation site in the mouse sequence and numbering on the left is relative to this +1 position. Arrows pointing to the right above the bold nucleotides in the mouse *CB1* sequence represent transcription start sites identified in this study. The arrow pointing to the right below the human *CB1* sequence represents the 5′-end of a human CB1 cDNA reported in GenBank. The downward pointing arrows indicate the position of the 5′-ends of mouse CB1 cDNA and EST clones that are present in GenBank. Exon sequence is indicated by upper case letters. The intronic sequences at the 5′- and 3′-splice site junctions are in lower case letters. The small dots represent 18 395 and 20 467 bp intron sequences in the mouse and human genomic DNA sequence, respectively, that separate the splice site sequences. The amino acid sequence of mouse and human CB1 encoded by exon 2 is shown above the aligned genomic sequences and the coding region is double underlined. Conserved transcription factor binding elements are underlined.

are affected by the expression of mutant huntingtin. When the function of this factor or synergistically acting group of factors is lost, there is no difference in CB1 expression throughout the striatum and cortex. It appeared that the length of the CAG repeat or relative expression levels of the *huntingtin* transgene affected the rate at which the function of this factor was lost in the two lines of transgenic HD mice.

The steady-state levels of CB1 mRNA could decrease in HD compared to wild-type mice if the rate of transcription was reduced or if mRNA turnover was increased. If CB1 mRNA stability was decreased, there would be a higher ratio of primary to mature transcript in striatal RNA isolated from HD compared to wild-type mice and the amount of unspliced primary transcript would be the same in wild-type and HD mice. If heteronuclear RNA splicing was affected by the expression of the human *HD* transgene, one would predict a relative increase in the amount of primary CB1 transcript at any given time point in HD mice as intron processing would be delayed and the half-life of the primary transcript would be increased. If transcription of the *CB1* gene decreased in a specific subset of neurons, the amount of primary and mature CB1 transcript would be lower in HD compared to wild-type mice. Moreover, the ratio of primary to mature transcript would be the same in both wild-type and HD mice after an equilibrium between

the new reduced rate of transcription and constant rate of turnover was established. We detected the primary transcript of the major CB1 transcription product in RPA analyses. There was less primary transcript detected in the R6/2 HD striatal RNA samples compared to wild-type striatal RNA samples as determined by densitometric analysis, and the ratio of primary to mature CB1 mRNA (approximately 0.1) was the same in the samples derived from wild-type and HD mice. To confirm the finding that the absolute levels of CB1 primary transcript were decreased in HD mouse striatum, we determined the levels of primary and mature CB1 mRNA by qRT-PCR. This analysis demonstrated that the rate of transcription of CB1 is reduced in the striatum of HD mice prior to the time that the decreased steady-state level of CB1 mRNA was observed.

An altered rate of transcription is consistent with the hypothesis that mutant huntingtin exerts its effects by altering transcription factor activity [5,21–24,31,32]. Comparative analysis of the promoter regions of the mouse and human *CB1* genes demonstrated that there were a number of transcription factor binding sites that have been conserved between the two species, suggesting that some common individual factor or groups of factors could be affected by the expression of mutant huntingtin in mice and humans. Only 1–2% of genes expressed in the striatum are affected by mutant huntingtin [18]. Mutant huntingtin and the transcription factors that have been shown to physically interact with mutant huntingtin are widely expressed throughout the brain. It is not yet known how mutant huntingtin selectively alters transcription of a small subset of genes by interacting with ubiquitously expressed transcription factors.

Another possibility is that mutant huntingtin itself has a characteristic that is unique when this protein is expressed in the striatum. It appears that with increasing age the length of the CAG repeat in mutant *HD* may be increased significantly by mechanisms that occur postmitotically [33,34]. Although the expression of *CB1* changes over time, the initial conditions that lead to the increased expression of *CB1* in the lateral striatum compared to elsewhere in the brain are present and functional in young HD mice. Loss of CB1 or other mRNAs and the development of NIIs and motor symptoms occur over time. It is possible that, due to the postmitotic change in the length of the CAG repeat, mutant huntingtin protein produced in the striatum of older animals may have significantly longer polyglutamine-repeats and have greater effects on transcription of a subset of genes in the striatum.

The toxic gain of function associated with mutant huntingtin is not restricted to transcriptional dysregulation. While the loss of individual gene products such as CB1 or any of the other mRNAs and proteins that have altered steady-state levels in the striatum of HD mice or patients likely contributes to disease progression, the inheritance and expression of mutant huntingtin is the primary cause of HD. Examination of the regulation of individual mutant huntingtin-affected genes such as *CB1* may increase our understanding of at least one abnormal function of mutant huntingtin by allowing us to identity the factor(s) that are affected by the expression of mutant huntingtin and the exact mechanism by which mutant huntingtin alters the function of such factors. This work describing the gene structure of *CB1* and its pattern of expression in transgenic mice will provide the information necessary to determine how mutant huntingtin alters the expression of this particular gene.

Acknowledgements

This work was supported by grants from the Canadian Institutes of Health Research to E. D.-W. and the Natural Sciences and Engineering Research Council of Canada (NSERC) to M.E.M.K. E.A.M. received an NSERC summer studentship. We thank M. Huang, K. Murphy and J. Nason for technical assistance.

References

1. Martin, J.B. & Gusella, J.F. (1986) Huntington's disease: pathogenesis and management. *N. Engl. J. Med.* **315**, 1267–1276.
2. The Huntington's Disease Collaborative Research Group (1993) A novel gene containing a trinucleotide repeat that is expanded and unstable on Huntington's disease chromosomes. *Cell* **72**, 971–983.
3. Trottier, Y., Biancalana, V. & Mandel, J.L. (1994) Instability of CAG repeats in Huntington's disease: relation to parental transmission and age of onset. *J. Med. Genet.* **31**, 377–382.
4. Duyao, M.P., Auerbach, A.B., Ryan, A., Persichetti, F., Barnes, G.T., McNeil, S.M., Ge, P., Vonsattel, J.P., Gusella, J.F., Joyner, A.L. & MacDonald, M.E. (1995) Inactivation of the mouse Huntington's disease gene homolog Hdh. *Science* **269**, 407–410.
5. Zuccato, C., Tartari, M., Crotti, A., Goffredo, D., Valenza, M., Conti, L., Cataudella, T., Leavitt, B.R., Hayden, M.R., Timmusk, T., Rigamonti, D. & Cattaneo, E. (2003) Huntingtin interacts with REST/NRSF to modulate the transcription of NRSE-controlled neuronal genes. *Nat. Genet.* **35**, 76–83.
6. Glass, M., Faull, R.L.M. & Dragunow, M. (1993) Loss of cannabinoid receptors in the substantia nigra in Huntington's disease. *Neuroscience* **56**, 523–527.
7. Richfield, E.K. & Herkenham, M. (1994) Selective vulnerability in Huntington's disease: preferential loss of cannabinoid receptors in lateral globus pallidus. *Ann. Neurol.* **36**, 577–584.
8. Glass, M., Dragunow, M. & Faull, R.L.M. (2000) The pattern of neurodegeneration in Huntington's disease: a comparative study of cannabinoid, dopamine, adenosine and $GABA_A$ receptor alterations in the human basal ganglia in Huntington's disease. *Neuroscience* **97**, 505–519.
9. Denovan-Wright, E.M. & Robertson, H.A. (2000) Cannabinoid receptor messenger RNA levels decrease in a subset of neurons in the lateral striatum, cortex and hippocampus of transgenic Huntington's disease mice. *Neuroscience* **98**, 705–713.
10. Mangiarini, L., Sathasivam, K., Seller, M., Cozens, B., Harper, A., Hetherington, C., Lawton, M., Trottier, Y., Lehrach, H., Davies, S. & Bates, G. (1996) Exon 1 of the HD gene with an expanded CAG repeat is sufficient to cause a progressive neurological phenotype in transgenic mice. *Cell* **87**, 493–506.
11. Naver, B., Stub, C., Moller, M., Fenger, K., Hansen, A.K., Hasholt, L. & Sorensen, S.A. (2003) Molecular and behavioral analysis of the R6/1 Huntington's disease transgenic mouse. *Neuroscience* **122**, 1049–1057.
12. Hebb, A.L.O., Robertson, H.A. & Denovan-Wright, E.M. (2004) Striatal phosphodiesterase mRNA and protein levels are reduced in Huntington's Disease transgenic mice prior to the onset of motor symptoms. *Neuroscience* **123**, 967–981.
13. Franklin, K.B.J. & Paxinos, G. (1997) *The Mouse Brain in Stereotaxic Coordinates*. Academic Press, San Diego.

14. Liu, R.Z., Denovan-Wright, E.M. & Wright, J.M. (2003) Structure, mRNA expression and linkage mapping of the brain-type fatty acid-binding protein gene (FABP7) from zebrafish (*Danio rerio*). *Eur. J. Biochem.* **270**, 715–725.
15. Matsuda, L.A., Lolait, S.J., Brownstein, M.J., Young, A.C. & Bonner, T.I. (1990) Structure of a cannabinoid receptor and functional expression of the cloned cDNA. *Nature* **346**, 561–564.
16. Gerard, C.M., Mollereau, C., Vassart, G. & Parmentier, M. (1991) Molecular cloning of a human cannabinoid receptor which is also expressed in testis. *Biochem. J.* **279**, 129–134.
17. Chakrabarti, A., Onaivi, E.S. & Chaudhuri, G. (1995) Cloning and sequencing of a cDNA encoding the mouse brain-type cannabinoid receptor protein. *DNA Seq.* **5**, 385–388.
18. Luthi-Carter, R., Strand, A.D., Peters, N.L., Solano, S.M., Hollingsworth, Z.R., Menon, A.S., Frey, A.S., Spektor, B.S., Penney, E.B., Schilling, G., Ross, C.A., Borchelt, D.R., Tapscott, S.J., Young, A.B., Cha, J.-H.J. & Olson, J.M. (2000) Decreased expression of striatal signaling genes in a mouse model of Huntington's disease. *Hum. Mol. Genet.* **9**, 1259–1271.
19. Luthi-Carter, R., Hanson, S.A., Strand, A.D., Bergstrom, D.A., Chun, W., Peters, N.L., Woods, A.M., Chan, E.Y., Kooperberg, C., Krainc, D., Young, A.B., Tapscott, S.J. & Olson, J.M. (2002) Dysregulation of gene expression in the R6/2 model of polyglutamine disease: parallel changes in muscle and brain. *Hum. Mol. Genet.* **11**, 1911–1926.
20. Proudfoot, N.J., Furger, A. & Dye, M.J. (2002) Integrating mRNA processing with transcription. *Cell* **108**, 501–512.
21. Steffan, J.S., Kazantsev, A., Spasic-Boskovic, O., Greenwald, M., Zhu, Y.-Z., Gohler, H., Wanker, E., Bates, G., Housman, D.E. & Thompson, L.M. (2000) The Huntington's disease protein interacts with p53 and CBP and represses transcription. *Proc. Natl Acad. Sci. USA* **97**, 6763–6768.
22. Dunah, A.W., Jeong, H., Griffin, A., Kim, Y.-M., Standaert, D.G., Hersch, S.M., Mouradian, M.M., Young, A.B., Tanese, N. & Krainc, D. (2002) Sp1 and TAFII130 transcriptional activity disrupted in early Huntington's disease. *Science* **296**, 2238–2243.
23. Li, S.-H., Cheng, A.L., Zhou, H., Lam, S., Rao, M., Li, H. & Li, X.-J. (2002) Interaction of Huntington's disease protein with transcriptional activator Sp1. *Mol. Cell. Biol.* **22**, 1277–1287.
24. Yohrling, G.J., Farrell, L.A., Hollenberg, A.N. & Cha, J.H.J. (2003) Mutant huntingtin increases nuclear corepressor function and enhances ligand-dependent nuclear hormone receptor activation. *Mol. Cell Neurosci.* **23**, 28–38.
25. Devane, W.A., Hanus, L., Breuer, A., Pertwee, R.G., Sevenson, L.A., Griffin, G., Gibson, D., Mandelbaum, A., Etinger, A. & Mechoulam, R. (1992) Isolation and structure of a brain constituent that binds to the cannabinoid receptor. *Science* **258**, 1946–1949.
26. Mechoulam, R., Ben-Shabat, S., Hanus, L., Ligumsky, M., Kaminski, N.E., Schatz, A.R., Gopher, A., Almog, S., Martin, B.R., Compton, D.R., Pertwee, R.G., Griffin, G., Bayewitch, M., Barg, J. & Vogel, Z. (1995) Identification of an endogenous 2-monoglyceride, present in canine gut, that binds to cannabinoid receptors. *Biochem. Pharmacol.* **50**, 83–90.
27. Glass, M. (2001) The role of cannabinoids in neurodegenerative diseases. *Prog. Neuro-Psychopharmacol. Biol. Psychiat.* **25**, 743–765.
28. Carter, R.J., Lione, L.A., Humby, T., Mangiarini, L., Mahal, A., Bates, G.P., Dunnett, S.B. & Morton, A.J. (1999) Characterization of progressive motor deficits in mice transgenic for the human Huntington's disease mutation. *J. Neurosci.* **19**, 3248–3257.
29. Hansson, O., Castilho, R.F., Korhonen, L., Lindholm, D., Bates, G.P. & Brundin, P. (2001) Partial resistance to malonate-induced striatal cell death in transgenic mouse models of Huntington's disease is dependent on age and CAG repeat length. *J. Neurochem.* **78**, 694–703.
30. Meade, C.A., Deng, Y.P., Fusco, F.R., Del Mar., N., Hersch, S., Goldowitz, D. & Reiner, A. (2002) Cellular localization and development of neuronal intranuclear inclusions in striatal and cortical neurons in R6/2 transgenic mice. *J. Comp. Neurol.* **449**, 241–269.
31. Cha, J.-H.J. (2000) Transcriptional dysregulation in Huntington's disease. *Trends Neurosci.* **23**, 387–392.
32. van Roon-Mom, W.M., Reid, S.J., Jones, A.L., MacDonald, M.E., Faull, R.L. & Snell, R.G. (2002) Insoluble TATA-binding protein accumulation in Huntington's disease cortex. *Brain Res. Mol. Brain Res.* **109**, 1–10.
33. Shelbourne, P.F., Killeen, N., Hevner, R.F., Johnston, H.M., Tecott, L., Lewandoski, M., Ennis, M., Ramirez, L., Li, Z., Iannicola, C., Littman, D.R. & Myers, R.M. (1999) A Huntington's disease CAG expansion at the murine Hdh locus is unstable and associated with behavioural abnormalities in mice. *Hum. Mol. Genet.* **8**, 763–774.
34. Kennedy, L. & Shelbourne, P.F. (2000) Dramatic mutation instability in HD mouse striatum: does polyglutamine load contribute to cell-specific vulnerability in Huntington's disease? *Hum. Mol. Genet.* **9**, 2539–2544.
35. Mathews, C.K., van Holde, K.E. & Ahern, K.G. (2000) *Biochemistry*, 3rd edn. Addison-Wesley Longman Inc, San Francisco, p. 1098.